J. Fluid Mech. (2000), *vol.* 421, *pp.* 293–305. Printed in the United Kingdom

Numerical simulation of convection and heat transfer in water absorbing solar radiation

By YU. G. VEREVOCHKIN[1] AND S. A. STARTSEV[2]

[1]Moscow State University for Geodesy and Cartography, Gorokhovskii 4, Moscow 103064, Russia

[2]Physical Lebedev Institute, Neutron Physics Department, Leninskii 53, Moscow 117924, Russia

(Received 5 May 1998 and in revised form 19 October 1999)

Thermal convection in a horizontal water layer being cooled from above and absorbing solar radiation is simulated numerically at the Prandtl number $Pr = 7$. Three different regimes arising are investigated here. The first is characterized by intermittent convection, the second by steady-state convection, and the third is convection free. The transitions occur at different values of J_0/Q, the ratio of downward solar-radiation flux just below the surface to heat flux through the interface (assumed to be constant), but at almost the same Rayleigh number. The generalized heat-conduction law is found to be valid.

1. Introduction

The effect of solar radiation and wind on both the evolution of an interfacial water layer and heat transfer in it was considered by Woods (1980), Paulson & Simpson (1981), Simpson & Dickey (1981*b*), and Soloviev & Schlüssel (1996). Similarly to Saunders (1967), Paulson & Simpson (1981) use formulae derived for radiation-free conditions and reduce the effect of solar radiation to a certain decrease in heat flux occurring just below the interface. Such an approach is questionable, at least when the case of zero wind speed is under consideration, because a mode of free convective motion and the qualitative structure of the interfacial water layer are fundamentally affected by solar radiation (see the calculations of Verevochkin & Startsev (1988) and laboratory experiment of Verevochkin, Il'in & Shevchenko (1990)). Although the approaches of the other authors mentioned above differ, they also have fundamental drawbacks in the case of zero wind speed that is under investigation here. For example, considering thermally driven convective instability of the layer, Woods uses a criterion derived for no downward irradiance and a constant temperature gradient. The model of Simpson & Dickey (1981*b*) contains the level-$2\frac{1}{2}$ version of the Mellor & Yamada (1974) turbulence closure scheme and is applied, in particular, in the case of zero wind speed. As is well-known, thermal convection can be in intermittent and steady-state regimes (see Foster 1971; Verevochkin & Startsev 1988, 1997). At a very high Rayleigh number, intermittent convection has, perhaps, some features of turbulence. However, steady-state cellular convection can hardly be treated as turbulence. Therefore, in the case of zero wind speed, the model under consideration should be applied with caution. Moreover, boundary conditions used in it, giving turbulent fluxes of heat and momentum, do not allow a description of the sublayer with molecular heat conduction dominating, which exists near the interface (see Soloviev & Schlüssel 1996). Soloviev & Schlüssel (1996) study the evolution of this interfacial conduction sublayer in the ocean during daytime. The model introduced is of the renewal type, where the renewal time of the sublayer is affected by absorbed solar radiation. The stability criterion used there to describe this effect is based on the ill-founded relation introduced by Woods (1980). The model is assumed to include, as a specific case, zero friction velocity when instability of the sublayer is of pure free-convection nature. However, then, the assumption used in the model that there is complete periodic destruction of the sublayer proves to be not correct (see Verevochkin & Startsev 1997). The approach discussed also excludes consideration of possible steady-state regimes of thermal convection.

Numerical simulation and laboratory experimental investigation of both convection and heat transfer in an interfacial water layer cooled from above and absorbing solar radiation were carried out by Verevochkin & Startsev (1988) and Verevochkin *et al.* (1990), respectively. However, the laboratory experiment was not precise enough to give quantitative data. Similarly, our previous numerical calculations (1988) were not sufficiently accurate, because they were carried out for infinite Prandtl number Pr.

Here, based on the model developed by us earlier (Verevochkin & Startsev 1997), we consider the evolution of an interfacial water layer and heat transfer occurring in it at zero wind speed and the Prandtl number typical for water ($Pr = 7$). The combined effect of surface cooling and absorption of solar radiation is investigated. Taking account of only two factors simplifies the problem and allows its accurate solution. On the other hand, the statement of the problem is rather general, because it is free from empirical relations. Therefore, our approach is applicable for any water basin under corresponding weather conditions. The effects of salinity and optical type of water are not investigated here.

The plane horizontally infinite water layer under consideration has both a free surface and a rigid bottom. Water undergoes deceleration both near the bottom and near the free surface. The first effect occurs due to the non-slip condition. The second is caused by the property of water to absorb surfactant substances, reducing its surface tension: when breaking the surfactant film and radially sweeping it out, an upward disturbance acquires higher surface tension, which counteracts its radial expansion (see Berg, Acrivos & Boudart 1966). As in our paper published in 1997, we model this deceleration by *decelerating sublayers* in which volume retarding forces are assumed to act. The sublayers are sufficiently thin that they do not distort the convective motion and the heat transfer. Moreover, parameters of the sublayers provide limit transitions to the non-slip boundary or to the elastic free surface: in a series of calculations, we increase the effectiveness of the deceleration and diminish the sublayer thickness as long as the solution obtained varies. The other details of the model used are conventional.

A model differing from that we shall use below in the absence of solar radiation has been successfully verified by the experimental results of Katsaros *et al.* (1977) (see Verevochkin & Startsev 1997). The latter paper shows that using decelerating sublayers for water confined by horizontal rigid plates also gives results that are in a good agreement with experimental data.

2. Mathematical model

Consider water as an incompressible fluid having constant properties except for the density as it affects the buoyancy term (the Boussinesq approximation). The equation of state is assumed to be linear. Let the length scale be equal to the depth of the fluid layer h; the time scale h^2/k, where k is the thermometric conductivity; and the temperature scale be $(Qh)/(\rho ck)$, where ρ is the density at some reference temperature,

c is the specific heat, and Q is the time-independent upward heat flux through the free surface. Divide the temperature T into a horizontal average $\bar{T}(z,t)$ and a fluctuating part $\theta(x,z,t)$ so that $T = \bar{T} + \theta$ and $\bar{\theta} = 0$. Then, a two-dimensional heat-conduction equation takes the following dimensionless form:

$$\frac{\partial \bar{T}}{\partial t} + \frac{\partial \theta}{\partial t} + u\frac{\partial \theta}{\partial x} + w\frac{\partial \theta}{\partial z} + w\frac{\partial \bar{T}}{\partial z} = \left(\frac{\partial^2}{\partial x^2} + \frac{\partial^2}{\partial z^2}\right)\theta + \frac{\partial^2 \bar{T}}{\partial z^2} + \frac{h}{Q}\dot{q}, \tag{1}$$

where x and z are the horizontal and vertical spatial coordinates, u and w are the horizontal and vertical velocity components, and $\dot{q}$ is the dimensional energy-release rate related to unit volume and caused by absorption of solar radiation.

The dimensional downward solar-radiation flux in water J is given by the formula

$$J = J_0 \sum_{i=1}^{9} D_i \exp(-z'/\xi_i), \tag{2}$$

where J_0 is the value of J just below the interface, z' is the dimensional vertical coordinate (the z-axis is downward), and D_i and ξ_i are as used by Defant (1961), Simpson & Dickey (1981*a*), and Paulson & Simpson (1981). As a result,

$$\dot{q} = -\frac{\mathrm{d}J}{\mathrm{d}z'} = J_0 \sum_{i=1}^{9} \frac{D_i}{\xi_i} \exp(-zh/\xi_i). \tag{3}$$

We also use the continuity equation

$$\frac{\partial u}{\partial x} + \frac{\partial w}{\partial z} = 0 \tag{4}$$

and the equation resulting from the Navier–Stokes equations (see Verevochkin & Startsev 1997)

$$\frac{1}{Pr}\frac{\partial}{\partial x}\left[\frac{\partial}{\partial t}\mathbf{rot}_y(\boldsymbol{v}) + \left(u\frac{\partial}{\partial x} + w\frac{\partial}{\partial z}\right)\mathbf{rot}_y(\boldsymbol{v})\right]$$
$$= R\frac{\partial^2 \theta}{\partial x^2} + \frac{\partial}{\partial x}\left(\frac{\partial^2}{\partial x^2} + \frac{\partial^2}{\partial z^2}\right)\mathbf{rot}_y(\boldsymbol{v}) + \beta(z)\left(\frac{\partial^2}{\partial x^2} + \frac{\partial^2}{\partial z^2}\right)w + \frac{\mathrm{d}\beta}{\mathrm{d}z}\frac{\partial w}{\partial z}. \tag{5}$$

Here, $\mathbf{rot}_y(\boldsymbol{v}) = \partial u/\partial z - \partial w/\partial x$ ($\boldsymbol{v}$ is the dimensionless velocity), Pr is the Prandtl number, and $R = \alpha g Q h^4/(\nu\rho c k^2)$ is the flux Rayleigh number, where α is the coefficient of thermal volume expansion, ν the kinematic viscosity, and g the acceleration due to gravity.

The terms in (5) that contain $\beta(z)$ describe the effect of a volume decelerating force introduced in our (1997) paper by the dimensional formula $\boldsymbol{F}' = -\beta'(z')\boldsymbol{v}'$. The dimensionless function $\beta(z) = (h^2/\nu\rho)\beta'(z')$ differs from zero only inside the decelerating sublayers and has the following form:

$$\beta(z) = \begin{cases} \beta_0 \cos^2(N_0 \pi z), & 0 \leqslant z \leqslant \dfrac{1}{2N_0} \quad \text{and} \quad 1 - \dfrac{1}{2N_0} \leqslant z \leqslant 1 \\ 0, & \dfrac{1}{2N_0} < z < 1 - \dfrac{1}{2N_0}. \end{cases} \tag{6}$$

Here, $1/2N_0$ is the dimensionless thickness of each decelerating sublayer (N_0 is an integer), and β_0 gives intensity of the deceleration.

To provide transition to the limits of both the non-slip boundary and the elastic free surface, β_0 and N_0 are chosen so that a further increase in intensity of the deceleration (increase in β_0) and a further decrease in thickness of the sublayers (increase in N_0) do not change the results of the calculations.

Water retardation in the decelerating sublayers adjacent to the bottom and the free surface allows application of the free boundary conditions for the velocity at both boundaries

$$w = \frac{\partial^2 w}{\partial z^2} = 0 \quad \text{at} \quad z = 0, 1 \tag{7}$$

and, consequently, expanding the velocity in the sine Fourier series

$$w = \sum_{n=1}^{N} A_n(t) \sin(n\pi z) \cos(ax). \tag{8}$$

Then, substituting (8) into the continuity equation (4) and solving for the horizontal velocity component u yields

$$u = -\sum_{n=1}^{N} A_n(t) \left(\frac{n\pi}{a}\right) \cos(n\pi z) \sin(ax). \tag{9}$$

The bottom is insulated, and the upward heat flux Q through the free surface is time- and horizontal-coordinate-independent. Thus,

$$\frac{\partial \theta}{\partial z} = 0 \quad \text{at} \quad z = 0, 1, \tag{10}$$

and

$$\frac{\partial \bar{T}}{\partial z} = 1 \quad \text{at} \quad z = 0, \quad \text{and} \quad \frac{\partial \bar{T}}{\partial z} = 0 \quad \text{at} \quad z = 1. \tag{11}$$

Boundary conditions (10) and (11) lead to the following expansions of θ and $\bar{T}$:

$$\theta = \sum_{n=0}^{N} C_n(t) \cos(n\pi z) \cos(ax), \tag{12}$$

$$\bar{T} = \frac{2}{\pi} \sum_{n=1}^{N} \frac{B_n(t)}{n} \cos(n\pi z) - (0.5z^2 - z + B_0(t)) - t. \tag{13}$$

The horizontal wavenumber a is chosen as that giving the largest value of the root-mean-square average of the vertical velocity at the point of the onset of convection (see Foster 1971). The procedure for deriving equations for the Fourier coefficients A_n, B_n, and C_n is similar to that presented in our (1997) paper. Substituting the expansions for w, u, and θ into (5), multiplying the equation obtained by $\sin(r\pi z)\cos(ax)$, and integrating the product from $x = 0$ to $x = 2\pi/a$ and from $z = 0$ to $z = 1$ yields

$$A_r'(t) = -Pr(a^2 + \pi^2 r^2) A_r(t) - \frac{2a^2 PrR}{a^2 + \pi^2 r^2} \sum_{n=0}^{N} C_n G_{nr}$$
$$-\frac{2Pr\beta_0}{a^2 + \pi^2 r^2} \left[\sum_{n=1}^{N} (a^2 + \pi^2 n^2) A_n b_{nrN_0} + \pi^2 N_0 \sum_{n=1}^{N} n A_n \bar{b}_{nrN_0} \right], \tag{14}$$

where

$$\bar{b}_{nrN_0} = \int_{1-1/(2N_0)}^{1} \cos(n\pi z)\sin(r\pi z)\sin(2\pi N_0 z)\,\mathrm{d}z + \int_{0}^{1/(2N_0)} \cos(n\pi z)\sin(r\pi z)\sin(2\pi N_0 z)\,\mathrm{d}z, \tag{15}$$

$$b_{nrN_0} = \int_{1-1/(2N_0)}^{1} \sin(n\pi z)\sin(r\pi z)\cos^2(\pi N_0 z)\,\mathrm{d}z + \int_{0}^{1/(2N_0)} \sin(n\pi z)\sin(r\pi z)\cos^2(\pi N_0 z)\,\mathrm{d}z, \tag{16}$$

and

$$G_{rn} = \int_0^1 \cos(r\pi z)\sin(n\pi z)\,\mathrm{d}z. \tag{17}$$

To derive equations for C_r, substitute (8), (9), (12), and (13) into (1), multiply the equation obtained by $\cos(r\pi z)\cos(ax)$ $(r \geqslant 0)$, and integrate the product from $x = 0$ to $x = 2\pi/a$ and from $z = 0$ to $z = 1$:

$$C_r'(t) = 4\sum_{n=1}^{N}\sum_{m=1}^{N} A_n(t)B_m(t)L_{nmr} + 2\sum_{n=1}^{N} A_n(t)S_{nr} - (a^2+\pi^2 r^2)C_r(t) \quad (r \geqslant 1), \tag{18}$$

$$C_0'(t) = \sum_{n=1}^{N} A_n(t)B_n(t) + \sum_{n=1}^{N} A_n(t)S_{n0} - a^2 C_0(t), \tag{19}$$

where

$$L_{nmr} = \int_0^1 \sin(n\pi z)\sin(m\pi z)\cos(r\pi z)\,\mathrm{d}z, \tag{20}$$

$$S_{nr} = \int_0^1 (z-1)\cos(r\pi z)\sin(n\pi z)\,\mathrm{d}z. \tag{21}$$

The above equations for A_r and C_r coincide with those derived in our (1997) paper for $J_0 = 0$. Terms containing J_0 arise only in equations for B_r. These equations also result from (1) in which the expansions for w, u, θ, and $\bar{T}$ are substituted. After the substitution, (1) is either integrated as formerly $(r = 0)$ or first multiplied by $\cos(r\pi z)$ and then integrated $(r \geqslant 1)$:

$$B_r'(t) = \frac{\pi^2 r}{2}\left[\sum_{m=1}^{N}\sum_{n=1}^{N} mA_nC_mL_{nmr} - \sum_{m=0}^{N}\sum_{n=1}^{N} nA_nC_mJ_{nmr}\right] - \pi^2 r^2 B_r(t) + \frac{\pi r h J_0}{Q}\sum_{i=1}^{9}\frac{D_i}{\xi_i}E_r(h/\xi_i) \quad (r \geqslant 1), \tag{22}$$

$$B_0'(t) = \frac{J_0}{Q}\left(\sum_{i=1}^{9} D_i \exp(-h/\xi_i) - 1\right), \tag{23}$$

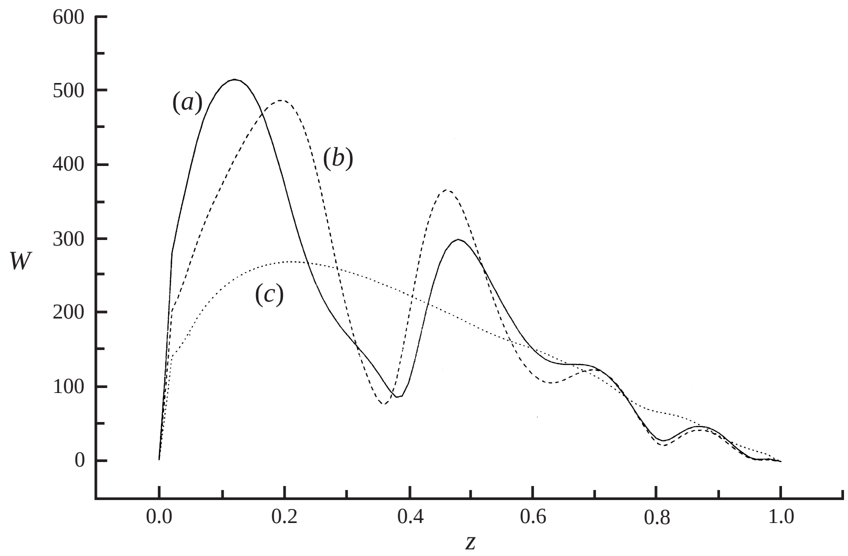

FIGURE 1. Vertical profiles of the horizontal root-mean-square average of dimensionless water velocity at different times for $R = 5 \times 10^8$, $N = 102$, $N_0 = 55$, $\beta_0 = 1.1 \times 10^6$, where (a, b) $J_0/Q = 1.5$, $a = 42.5$; (c) $J_0/Q = 1.9$, $a = 41.5$.

where

$$J_{nmr} = \int_0^1 \cos(n\pi z)\cos(m\pi z)\cos(r\pi z)\,\mathrm{d}z, \tag{24}$$

$$E_r(y) = \int_0^1 \cos(r\pi z)\exp(-yz)\,\mathrm{d}z. \tag{25}$$

To solve the system of ordinary differential equations for A_r, B_r, and C_r, we begin with an isothermal fluid and very small 'white-noise' θ, that is, with $B_r(0) = 1/\pi r$ $(r \geqslant 1)$, $B_0 = 1/3$, and $C_0(0) = 10^{-10}$. Initial values of A_r are found from the condition $\partial u/\partial t = \partial w/\partial t = 0$.

3. Results and discussion

Obviously, at small values of J_0, the convection has the intermittent character described by Foster (1971) for $Pr = \infty$ and $J_0 = 0$, by Verevochkin & Startsev (1988) for $Pr = \infty$ and small J_0, and by Verevochkin & Startsev (1997) for $J_0 = 0$ and $Pr = 4.3$–11. Then, the unstable decrease in water temperature that arises near the free surface (the cool skin) causes the onset of convection there, and the maximum of the vertical distribution of the horizontal root-mean-square average of fluid velocity proves to be not far from the interface (figure 1, curve a). Being intensified with time, the convection partly destroys the cool skin when a blob of cold water begins to move downward (figure 1, curve b). After that, the cool skin is restored, and the process repeats itself. In this regime, the temperature drop across the cool skin, which represents a drop in surface temperature with respect to the temperature maximum that exists, practically always, under the interface at $J_0 \neq 0$ (see figures 3 and 5b), is a random function of time (figure 2, curve a), and the vertical profile of the temperature $\bar{T}(z)$ has a dip corresponding to a convective cell formed near the interface (figure 3). A heat-conduction law, which is valid here, generalizes the conventional expression

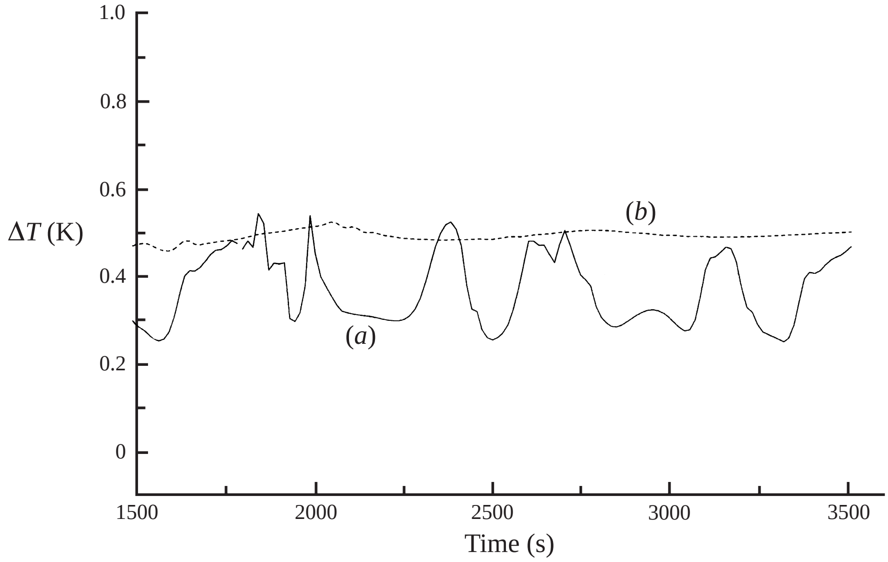

FIGURE 2. Horizontal-average dimensional temperature drop across the cool skin at $Q = 100\,\mathrm{W\,m^{-2}}$, $R = 5 \times 10^8$, $N = 102$, $N_0 = 55$, $\beta_0 = 1.1 \times 10^6$, where (*a*) $J_0/Q = 1.5$, $a = 42.5$; (*b*) $J_0/Q = 1.9$, $a = 41.5$.

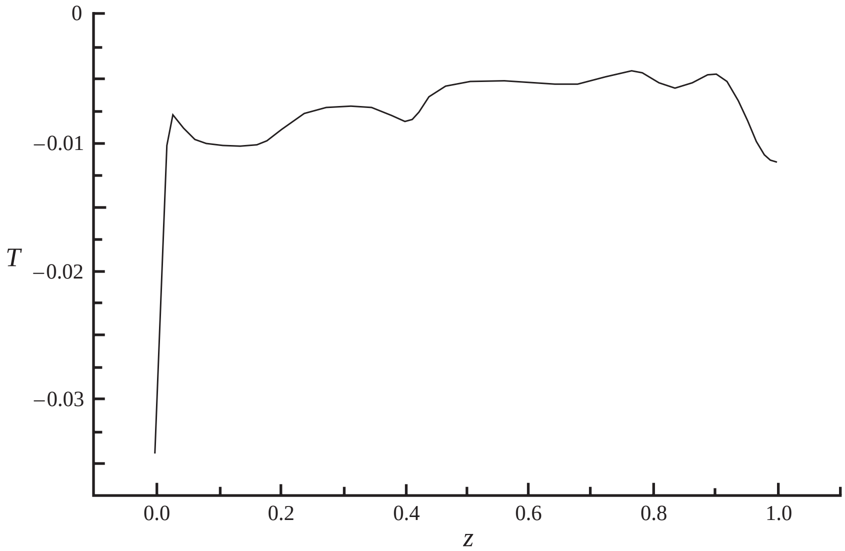

FIGURE 3. Vertical profile of the horizontal-average dimensionless water temperature at $J_0/Q = 1.5$, $R = 5 \times 10^8$, $N = 102$, $N_0 = 55$, $\beta_0 = 1.1 \times 10^6$, $a = 42.5$.

obtained for $J_0 = 0$. It has the form

$$Nu = ARa^n f(J_0/Q), \tag{26}$$

where

$$Nu = \frac{Qz'_m}{\rho c k \Delta T'} \tag{27}$$

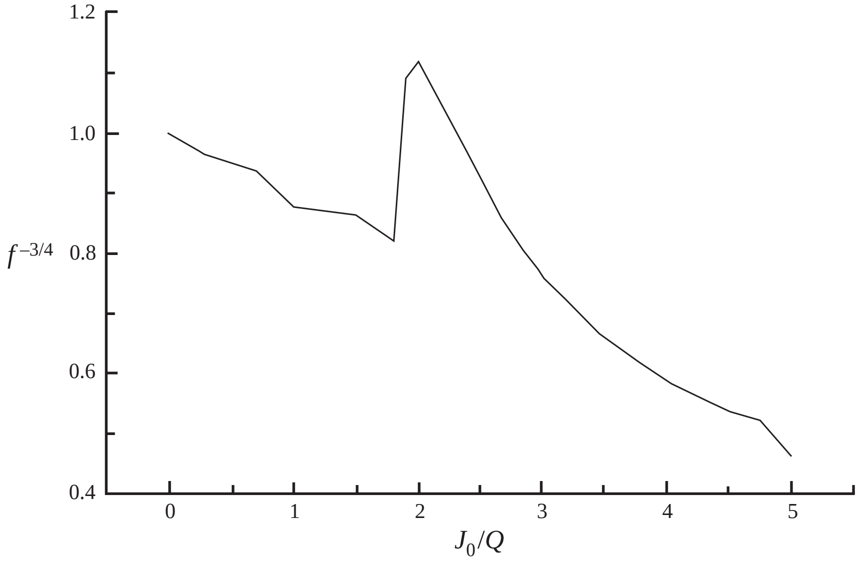

FIGURE 4. Function correcting the heat-conduction law to a power of $-\frac{3}{4}$.

is the Nusselt number,

$$Ra = \frac{\alpha g \Delta T' {z'_m}^3}{k\nu} \tag{28}$$

is the Rayleigh number, $f(0) = 1$, $\Delta T'$ is the time-average temperature drop across the cool skin, and z'_m is the time-average depth of the undersurface temperature maximum.

A law of the form (26) was verified by Katsaros *et al.* (1977) in a laboratory investigation of heat transfer in water having a free surface at $J_0 = 0$ ($f = 1$). As in other works considering water under such conditions, Q was treated as the time-average heat flux through the interface, which was determined by measuring an average rate of water cooling, while $\Delta T'$ and z'_m represented an average temperature drop across the entire water layer and the total thickness of this layer, respectively. When simulating heat transfer in water under such conditions, we assumed that Q was constant (see Verevochkin & Startsev 1997). Although this assumption seems to contradict the fluctuating character of the temperature drop, we succeeded in reproducing both the n and A measured by Katsaros *et al.* (1977). Here, we also consider Q as constant, especially as absorbed solar radiation reduces temperature fluctuations. The assumption that $Q = \text{const}$ during the time period between successive renewals of the conduction sublayer was also used by Soloviev & Schlüssel (1996). In contrast with our previous calculations (1997), we introduce Ra and Nu for the skin, but not for the entire water layer (here and below, the meaning of $\Delta T'$ and z'_m is that given to them just below formula (28)). We do this because a temperature drop across the cool skin either fluctuates with respect to some average value or has a small monotonic variation even at large J_0/Q whereas the temperature drop across the entire water layer can grow abruptly. As a result, according to our calculations, $n = \frac{1}{3}$ and $A = 0.215$ so that the latter quantity differs from the one calculated by us earlier (1997) for the entire water layer and $J_0 = 0$.

In the regime under consideration, an increase in J_0/Q causes a decrease in $\Delta T'$ and, consequently, in $f^{-3/4}(J_0/Q)$ (figure 4) due to a decrease in water cooling (from

(26), $\Delta T' \sim f^{-3/4}$). However, when J_0/Q reaches 1.8, the mode of convective motion changes abruptly. As a result, at $J_0/Q \geqslant 1.9$, the convection is almost steady state, and the maximum of the horizontal root-mean-square average of the dimensionless total velocity W is shifted downward compared to its position at the point of the cool-skin instability (figure 1, curves *a* and *c*). This transition probably occurs when the temperature drop across the cool skin becomes too small to maintain the convective circulation. As a result, the convection becomes less intense, and its generation region spreads to occupy a zone with a higher temperature drop (figure 1, curve *c*). Weakening of the convection and its shifting downward, in turn, increase the temperature drop across the cool skin and, consequently, the function $f^{-3/4}$ in the region of the transition (figure 4).

After the transition, this temperature drop is a smooth function of time (figure 2, curve *b*), and, except for a small region at the top of the water layer, the temperature gradient is almost constant in the convection zone (figure 5). The convective layer is larger than the sublayer of thermal compensation but, as a function of J_0/Q, varies in the same direction (figure 5*a*). Note that, according to Woods (1980), the sublayer of thermal compensation absorbs solar radiation at a rate equal to that of surface loss.

The problem of stability of a water layer under the conditions considered here has not been solved yet. However, a similar problem has been studied in the absence of incident solar radiation. Spangenberg & Rowland (1961) investigated experimentally convection in water subjected to evaporative cooling. They obtained that the critical Rayleigh number Ra_{cr} necessary for maintaining convection was equal to 102. However, their result depends strongly on thickness of the cooled layer having an indefinite lower boundary. Therefore, it is desirable to find a method of obtaining Ra_{cr} that is independent of the position of this boundary. Such a method was proposed by Ginzburg & Fedorov (1978). It is based on the relationship

$$Nu = ARa^{1/3} \tag{29}$$

applied for instantaneous values of Nu and Ra so that the onset of convection corresponds to $Nu = 1$. Then, the critical Rayleigh number $Ra_{cr} = A^{-3}$. If we use $A = 0.156$ as measured by Katsaros *et al.* (1977), calculated by us (1997), and related to the entire water layer, then $Ra_{cr} = 263$. This value is close to the transitional Rayleigh number $Ra_1 = 280$ corresponding to the change of the mode of convection ($J_0/Q = 1.8$) and calculated here using the temperature drop across the cool skin $\Delta T'$ and the thickness of this skin z'_m. However, using the $A = 0.215$ calculated here for the cool skin gives a value of Ra_{cr} equal to 100, which differs substantially from Ra_1 but is close to the value obtained by Spangenberg & Rowland (1961).

Consider the regimes arising for $J_0/Q > 2$ in more detail. As J_0/Q increases, the convection (figure 5*a*) becomes less intense, occupies a thinner layer and, finally, disappears. Simultaneously, the constant temperature gradient being formed in the convective zone first decreases (figure 5*b*), then changes its sign, and, at sufficiently low intensity of the convection, disappears (figure 6). All these transformations occur smoothly without jumps. Figure 7(*a*) presents the root-mean-square average of the dimensionless vertical velocity

$$W^* = \left(\int_0^1 \langle w^2 \rangle \, \mathrm{d}z \right)^{1/2} \tag{30}$$

(the angular brackets $\langle \ldots \rangle$ denote averaging over x) calculated for the entire water

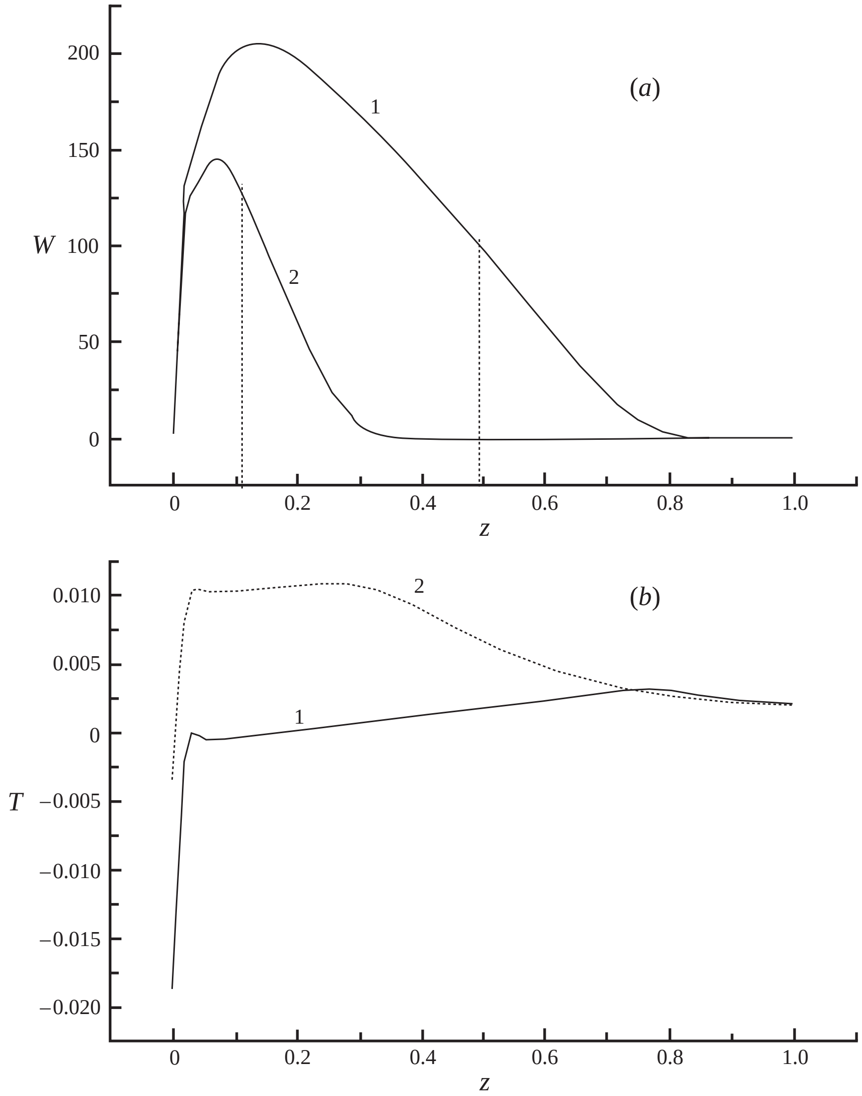

FIGURE 5. Vertical profiles of (a) the horizontal root-mean-square average of dimensionless water velocity and (b) the horizontal-average dimensionless water temperature at $R = 5 \times 10^8$, $N = 102$, $N_0 = 55$, $\beta_0 = 1.1 \times 10^6$: (1) $J_0/Q = 2.6$, $a = 40.4$; (2) $J_0/Q = 3.5$, $a = 37.8$. In each case, dotted lines bound the sublayers of thermal compensation.

layer as a function of J_0/Q. The corresponding function $\mathrm{d}W^*/\mathrm{d}(J_0/Q)$ is plotted in figure 7(b). It is natural to assume that the convection vanishes at a point where the function $\mathrm{d}W^*/\mathrm{d}(J_0/Q)$ has its minimum. This gives the value 4.8 for the transitional ratio J_0/Q. The corresponding transitional Rayleigh number Ra_2 calculated by using both an average drop in the temperature at the surface with respect to its value at the undersurface maximum and the thermal-compensation depth takes the value 252. Below, we discuss the reasons for choosing these scales.

Intermittent convection is generated in a thin unstably stratified layer, which is bounded by the interface and the average depth of the undersurface temperature maximum. Therefore, the thickness of this layer z_m' represents the spatial scale of the

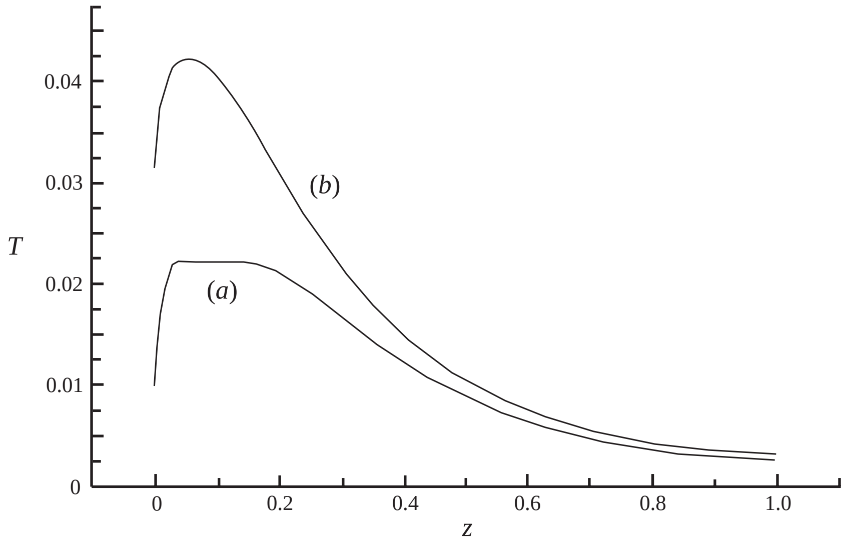

FIGURE 6. Vertical profiles of the horizontal-average dimensionless water temperature at $R = 5 \times 10^8$, $N = 102$, $N_0 = 55$, $\beta_0 = 1.1 \times 10^6$: (*a*) $J_0/Q = 4$, $a = 36.7$; (*b*) $J_0/Q = 4.75$, $a = 34.8$.

phenomenon. If intermittent convection occurs, then, following an increase in J_0/Q, Ra defined with the use of z'_m (see (28)) falls to Ra_1 ($J_0/Q = 1.8$). Then, transition to the steady-state regime takes place. As a result, $\Delta T'$ increases, while z'_m reduces slightly so that $Ra = Ra_1$ up to $J_0/Q = 2$. Further increase in J_0/Q causes some growth of Ra ($\Delta T'$ decreases, while z'_m slightly increases), which, at $J_0/Q = 3$, is equal to 359 and, at $J_0/Q = 4$, approaches 400. Although $Ra > Ra_1$ here, the steady-state convection that has developed suppresses the intermittent regime. Moreover, Ra defined with the use of z'_m does not characterize the steady-state convection, because it develops in a thicker layer. Nevertheless, if the heat-conduction law (26) is under consideration, any spatial scale, including z'_m, can be used, because, for $n = 1/3$, this law is independent of a spatial scale, which occurs to the same power on both sides and, consequently, can be cancelled. However, if we want to characterize the steady-state convection itself, a proper spatial scale should be chosen. Since convection cannot be generated outside the cooled layer, it is natural to take the thermal-compensation depth as such a scale, which we have done when defining Ra_2. The Rayleigh number Ra calculated for this scale decreases with increasing J_0/Q till the latter reaches the value 4.8. After that, at $Ra = Ra_2$, convection vanishes. The closeness of $Ra_1 = 280$ to $Ra_2 = 252$ is especially remarkable in view of their strong dependence on the spatial scale. So, substituting $z'_m = 0.032h$, which represents the average depth of the temperature maximum occurring under the interface at $J_0/Q = 1.8$ and is used for calculating Ra_1, by $z'_m = 0.031h$ changes the value of Ra_1 from 280 to 255. As our calculations are of some finite accuracy, the above-mentioned closeness may be treated as Ra_1 being equal to Ra_2. Consequently, the number (252–280) represents the minimum value of Ra that is necessary for maintaining both modes of convection in water that is absorbing solar radiation.

Soloviev & Schlüssel (1996) have calculated that, at zero friction velocity and $J_0/Q \approx 7$ or 14, the time-average difference between the temperature of the surface and that of the lower boundary of the conduction sublayer is positive. According to our calculations, for $J_0/Q \geqslant 3$, the quantity $\bar{T}(0,t)-\bar{T}(1,t)$ ($z = 1$ is the dimensionless

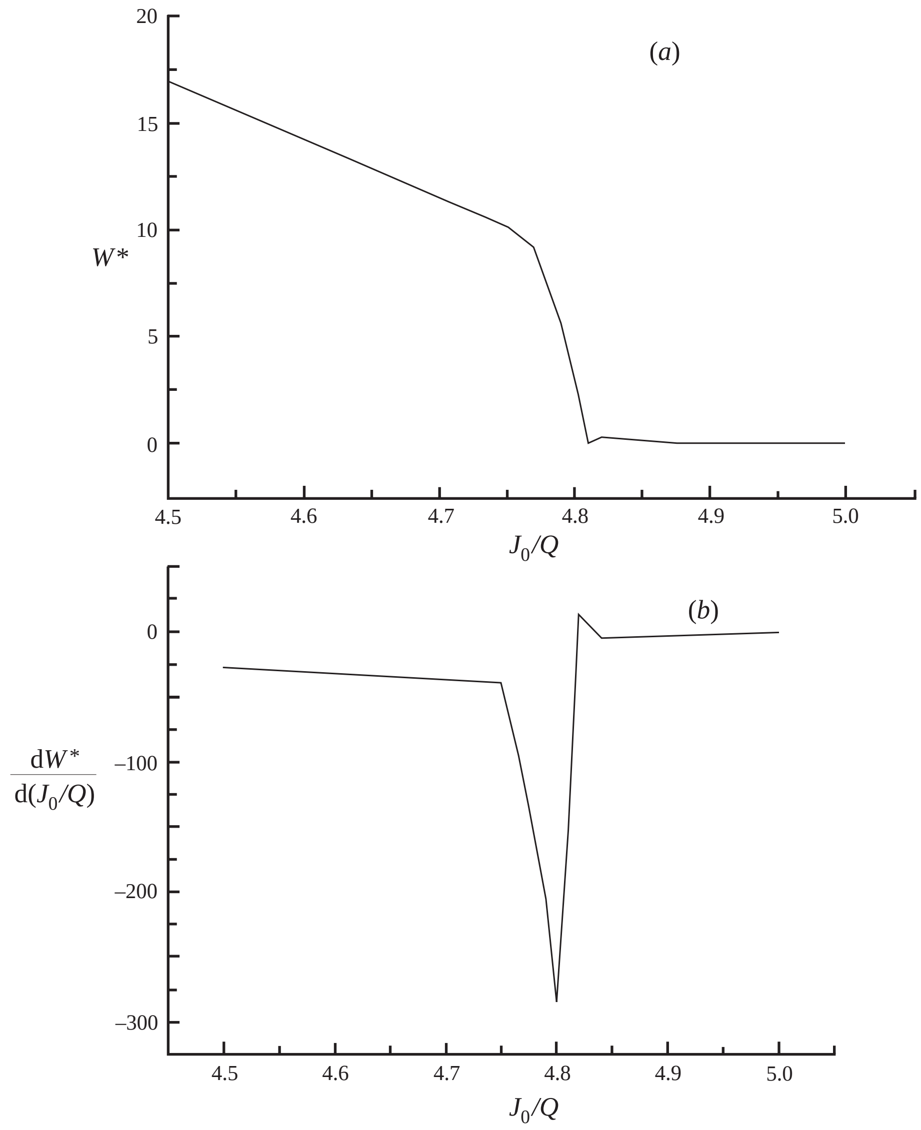

FIGURE 7. (*a*) Root-mean-square average of the dimensionless vertical water velocity and (*b*) its derivative with respect to J_0/Q both as a function of J_0/Q.

thickness of the total water layer) can become positive after a while, although the temperature does not drop just below the interface here (figure 6). Moreover, both models predict qualitatively different behaviour of the thermal boundary layer under such conditions: the model of Soloviev & Schlüssel (1996), which was developed for salt water, *a priori* assumes complete periodic destruction of the conduction sublayer, at least by salinity-driven convection. According to our model, which was developed for upward heat flux and fresh water, the temperature first grows with increasing depth and only then drops (figure 6); the undersurface temperature increase is practically time-independent; the convection either is steady state ($3 \leqslant J_0/Q \leqslant 4.8$) or vanishes ($J_0/Q > 4.8$); the surface-bulk temperature difference ($\bar{T}(0,t) - \bar{T}(1,t)$) grows monotonically with time.

The laboratory experiment in which a shielding film was used to make Q constant (Verevochkin *et al.* 1990) reveals two qualitatively different states of the interfacial boundary layer. The first state is similar to that observed here at $J_0/Q \leqslant 1.8$, while the second resembles regimes modelled by us at $J_0/Q \geqslant 2$. The transition between these states occurred at $J_0/Q \approx 3$. However, this value of J_0/Q is not reliable due to the low precision of measuring Q.

4. Conclusion

Three states of the interfacial boundary layer are simulated numerically in water that is cooled from above and absorbs solar radiation. The first state is characterized by intermittent convection; the second, by steady-state convection; and the third, is convection-free. The transition between the first two states is accompanied by a jump-like increase in the temperature drop across the cool skin, while the second transition is smooth. Both transitions occur at different values of J_0/Q but at almost the same value of the Rayleigh number ($Ra_1 = 280$ and $Ra_2 = 252$), which, in each case, has characteristic spatial scale of a different nature. The generalized heat-conduction law (26) is valid for all these states, where the function $f^{-3/4}(J_0/Q)$ is shown in figure 4.

REFERENCES

Berg, J. C., Acrivos, A. & Boudart, M. 1966 Evaporative convection. *Adv. Chem. Engng* **6**, 105.

Defant, A. 1961 *Physical Oceanography*, vol. 1, p. 53. Pergamon.

Foster, T. D. 1971 Intermittent convection. *Geophys. Fluid Dyn.* **2**(3), 201–217.

Ginzburg, A. I. & Fedorov, K. N. 1978 On a critical boundary Rayleigh number for water cooled through its free surface. *Izv. Akad. Nauk SSSR, Fiz. Atmos. Okeana* **4**, 433–435.

Katsaros, K. B., Lui, W. T., Businger, J. A. & Tillman, J. A. 1977 Heat transport and thermal structure in the interfacial boundary layer measured in an open tank of water in turbulent free convection. *J. Fluid Mech.* **83**, 311–335.

Mellor, G, L. & Yamada, T. 1974 A hierarchy of turbulence closure models for planetary boundary layers. *J. Atmos. Sci.* **31**, 1791–1806.

Paulson, C. A. & Simpson, J. J. 1981 The temperature difference across the cool skin of the Ocean. *J. Geophys. Res.* **86**(C11), 11044–11054.

Saunders, P. M. 1967 The temperature at the ocean-air interface. *J. Atmos. Sci.* **24**, 269–273.

Simpson, J. J. & Dickey, T. D. 1981*a* Alternative parametrizations of downward irradiance and their dynamical significance. *J. Phys. Oceanogr.* **11**, 876–882.

Simpson, J. J. & Dickey, T. D. 1981*b* The relation between downward irradiance and upper ocean structure. *J. Phys. Oceanogr.* **11**, 309–323.

Soloviev, A. V. & Schlüssel, P. 1996 Evolution of cool skin and direct air-sea gas transfer coefficient during daytime. *Boundary-Layer Met.* **77**, 45–68.

Spangenberg, W. G. & Rowland, W. R. 1961 Convective circulation in water induced by evaporative cooling. *Phys. Fluids* **4**, 743–750.

Verevochkin, Yu. G., Il'in, Yu. A. & Shevchenko, V. I. 1990 Laboratory investigation of a thermal boundary layer formed in water in sunny calm weather. *Izv. Akad. Nauk SSSR, Fiz. Atmos. Okeana* **26**, 301–306 [English transl. *Izv. Acad. Sci., Atmos. Ocean. Phys.* **26**(3), 219–223].

Verevochkin, Yu. G. & Startsev, S. A. 1988 Mathematical modeling of a thermal boundary layer formed in water in calm sunny weather. *Izv. Akad. Nauk SSSR, Fiz. Atmos. Okeana* **24**(10), 1100–1106 [English transl. *Izv. Acad. Sci., Atmos. Ocean. Phys.* **24**(10), 803–807].

Verevochkin, Yu. G. & Startsev, S. A. 1997 Use of decelerating sublayers in numerical simulation of gravity convection and heat transfer in a horizontal water layer. *Physica Scripta* **55**, 728–734.

Woods, J. D. 1980 Diurnal and seasonal variation of convection in the wind-mixed layer of the ocean. *Q. J. R. Met. Soc.* **106**, 379–394.